

# Asymmetric Spin Echo Sequences

## A Simple New Method for Obtaining NMR $^1\text{H}$ Spectral Images

DUANE D. BLATTER, MD,\* ALAN H. MORRIS, MD,\* DAVID C. AILION, PhD,†  
ANTONIO G. CUTILLO, MD,\* AND THOMAS A. CASE, BS†

Blatter DD, Morris AH, Ailion DC, Cutillo AG, Case TA. Asymmetric spin echo sequences: a simple new method for obtaining NMR  $^1\text{H}$  spectral images. *Invest Radiol* 1985;20:845-853.

The nuclear magnetic resonance (NMR) signal decay produced by reversible tissue-induced dephasing of the magnetization components in the transverse plane (reversible tissue-induced dephasing) was measured and expressed as a function of a new transverse relaxation time  $T_2'$  ( $T_2$  prime) for samples of rat liver, retroperitoneal fat, inflated lung, and corn oil. Simple exponentials did not adequately describe the observed NMR signal decay. Inflated lung demonstrated the most rapid signal decay ( $T_2' = 4.8$  ms) followed by retroperitoneal fat ( $T_2' = 16$  ms). No reversible tissue-induced dephasing was observed in liver ( $T_2'$  immeasurably long). In tissues which contain both fat and water, the chemically shifted  $^1\text{H}$  resonance peaks from -OH and -CH- are in phase with symmetric spin echo sequences but out of phase with asymmetric sequences. The interference of these two peaks produces a beat pattern with asymmetric sequences. Subtraction images obtained from paired symmetric- and asymmetric-sequence images accurately ( $r = .96$ ) reflect  $T_2'$  and can be used to indicate the presence of fat. In vivo subtraction images of ethionine-induced fatty rat livers were significantly different from similar in vivo images of normal rat livers ( $P < .0005$ ). Since for each pixel of a subtraction image, the magnitude of the difference signal should be approximately proportional to the ratio of hydroxyl and alkyl protons, this simple spin echo sequence modification may obviate the need for more time-consuming 3-dimensional Fourier transform proton chemical shift images.

**Key words:** nuclear magnetic resonance, chemical shift; nuclear magnetic resonance, tissue characterization; liver, fatty; lung aeration.

From the \*Division of Respiratory, Critical Care, and Occupational (Pulmonary) Medicine, Department of Internal Medicine, †Department of Physics, University of Utah and the LDS Hospital, Salt Lake City, Utah.

Preliminary oral reports of this work were presented at the 6th Specialized Ampere Conference, Crete, Greece, September 1983, and at the XXIInd Ampere Congress, Zurich, Switzerland, September 1984.

Supported by National Heart Lung and Blood Institute grants RO1-HL-23746 and RO1-HL-31216.

The authors thank Donald A. Eckard, MD, for technical and experimental assistance; Dennis Parker, PhD, and Keith Tolman, MD, for advice given; and Mr. Keith D. Green for secretarial assistance. We are also grateful to Don Alderman, PhD, and the University of Utah Department of Chemistry for allowing us use of their Varian 300 SC spectrometer.

Reprint requests: Alan H. Morris, MD, Pulmonary Division, LDS Hospital, Salt Lake City, Utah 84143.

Received May 14, 1984, and accepted for publication, after revision, May 29, 1985.

DIFFERENCES in the longitudinal ( $T_1$ ) and transverse ( $T_2$ ) relaxation times account for much of the current success of nuclear magnetic resonance (NMR) imaging techniques that distinguish pathologic from normal tissues.<sup>1-4</sup> In vivo spectroscopy provides additional diagnostic information. Images have recently been produced with such spectral information associated with each pixel, but the increase in imaging time is significant.<sup>5</sup> We describe herein the use of temporally asymmetric spin echo pulse sequences that produce images containing spectral information. Paired symmetric (conventional) and asymmetric images allow determination of the relative amounts of water and alkyl protons at each pixel of an image without the production of a complete proton spectrum and the consequent increase in imaging time.

Transverse or spin-spin relaxation produces a decay in the observed NMR signal due to dephasing of the magnetization components in the transverse or  $90^\circ$  plane. Magnetic field inhomogeneities and the consequent differences in the precession frequencies of the nuclei are the cause of the dephasing. The rate of NMR signal loss due to dephasing of the transverse magnetization components after a  $90^\circ$  pulse is described by the time  $T_2^*$  ( $T_2$  star) and is the summation of the contributions from all sources of magnetic field inhomogeneities including those arising from the externally applied magnetic field and those internal to the sample. There is a fundamental difference between that part of the NMR signal loss which is recovered after the application of a  $180^\circ$  pulse and that part which is not recovered (irreversibly lost). The transverse relaxation time,  $T_2$ , describes the rate of irreversible NMR signal loss. We have recently reported the observation of tissue-induced static magnetic field inhomogeneities whose contribution to the total transverse dephasing time constant,  $T_2^*$ , is recovered following the application of a  $180^\circ$  pulse.<sup>6</sup> We first observed this phenomenon in inflated lung tissue, and we hypothesized that the differing diamagnetic susceptibilities of air and water result in internal magnetic field inhomogeneities because of lung air-tissue interfaces.<sup>7</sup> We also observed a recoverable NMR signal loss in fat, but its mechanism was less clear.<sup>6</sup>

In this report, we measure the NMR signal decay due to reversible tissue-induced dephasing of the magnetization components in the transverse plane (reversible tissue-induced dephasing) and describe this signal decay as a function of time by empirical mathematical expressions. We call the time characterizing this signal decay  $T_2'$  ( $T_2$  prime; see reference 6 for details). The signal loss characterized by these expressions is similar to the signal loss in liquids arising from inhomogeneities in the external fields in that both are recoverable in a spin echo. The important difference is that the decay described herein arises from internal tissue sources of magnetic field inhomogeneity. We have observed this signal decay only in inflated lung and in tissues containing fat. We have taken advantage of this observation and produced images with marked enhancement of aerated lung and fat by utilizing paired symmetric and asymmetric spin echo sequences.<sup>6,7</sup> We also report herein the source of recoverable NMR signal loss in fat and demonstrate its utility in producing images of fatty liver. In addition, we demonstrate quantitatively that the signal loss associated with asymmetric spin echo sequences is in fact another manifestation of reversible tissue-induced dephas-

ing of the magnetization components in the transverse plane (reversible tissue-induced dephasing).

### Methods

NMR images were obtained using a Varian iron core magnet (12" pole face) modified for small animal imaging. The system operates at a field of 0.94 Tesla corresponding to a proton resonance of 40 MHz. Room temperature shim coils provide a field homogeneity of 0.1 gauss (10 ppm) over a volume of approximately 20 cm<sup>3</sup>, and field-locking circuitry effectively eliminates both short- and long-term drift. A spin echo line scan technique<sup>6</sup> similar to that described elsewhere<sup>7</sup> is employed. The line-scan technique involves the application of three perpendicular magnetic field gradients and 90° and 180° radio frequency pulses (spin echo technique) so as to excite the nuclei in one line through the specimen. The specimen and field gradients were arranged so that the line of excited nuclei was located in the homogeneous portion of the magnetic field. The specimen's position was then shifted slightly and the process repeated to excite a neighboring line of atoms. We thus obtained an entire slice with data taken from nuclei when they were all in the homogeneous portion of the field.

We refer to a spin echo sequence as symmetric if the time,  $\tau$ , from the center of the 90° pulse to the center of the 180° pulse is equal to the time,  $\tau'$ , from the center of the 180° pulse to the center of the spin echo (Fig. 1 and Table 1). If these parameters are not met, we refer to the sequence as asymmetric. The magnitude of temporal asymmetry,  $a$ , is defined as  $a = |\tau - \tau'|$  and will be noted in parentheses following the word "asymmetric" in both text and Table 1. Paired symmetric and asymmetric (2, 4, and 6 ms) sequence images were obtained of in vitro tissue samples and living (sedated) rats. The images obtained with asymmetric sequences were subtracted, pixel by pixel, from the corresponding images obtained with the symmetric sequence. This difference signal  $D$  was normalized, for each pixel, by expressing it as a fraction of the maximum NMR signal (obtained with the symmetric spin echo sequence). Thus,

$$D = \frac{\text{NMR symmetric signal} - \text{NMR asymmetric signal}}{\text{NMR symmetric signal}} \quad (1)$$

A subtraction image was then composed of these normalized difference signals ( $D$ ). In such an image, tissues with reversible tissue-induced dephasing appear white. All other tissues, as well as areas of no signal (air), appear black. Since both symmetric and asymmetric-sequence images were obtained with the same echo delay and the same repetition time, they are affected identically by  $T_1$  and  $T_2$  effects, and the subtraction images are then

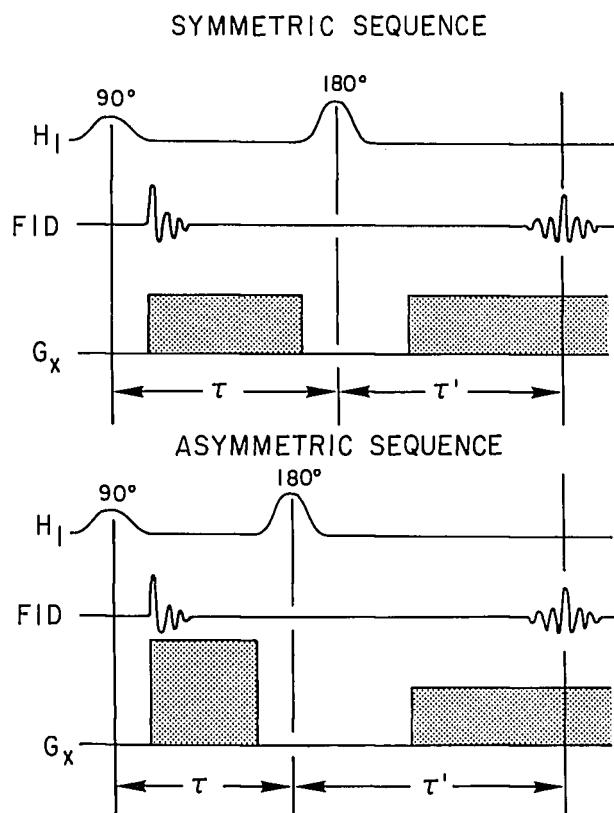


Fig. 1. Symmetric and asymmetric spin echo sequences. Spin echo occurs when the cross-hatched area under the x-gradient curve prior to the 180° pulse equals the cross-hatched area after the 180° pulse. Gradients in the y and z directions not shown. A symmetric sequence is defined as meeting the condition  $\tau = \tau'$ . Conversely, any sequence where  $\tau \neq \tau'$  is asymmetric.

TABLE 1. Symmetric and Asymmetric Spin Echo Sequence Times

Image Sequence	$\tau$	$\tau'$	Echo Delay (ms) = $\tau + \tau'$	Asymmetry (ms) $a =  \tau - \tau' $
Symmetric	9*	9†	18	0
Asymmetric (2 ms)	8	10	18	2
Asymmetric (4 ms)	7	11	18	4
Asymmetric (6 ms)	6	12	18	6
Asymmetric (8 ms)	5	13	18	8

\* $\tau$  = time (ms) from the center of the 90° pulse to the center of the 180° pulse (see Fig. 1).

† $\tau'$  = time (ms) from the center of the 180° pulse to the center of the spin echo (see Fig. 1).

independent of both  $T_1$  and  $T_2$  (echo delay =  $\tau + \tau' = 18$  ms [Fig. 1 and Table 1], repetition time = 1.0 sec).

Fatty liver in rats was produced by the administration of ethionine, an inhibitor of lipoprotein synthesis. Maximum accumulation of lipid after administration of ethionine is reported to occur between 24 and 48 hours.<sup>9</sup> Four virgin female Sprague-Dawley rats weighing 170 to 190 g received a single intraperitoneal injection of 300 mg of DL-Ethionine (Aldrich Chemical Company, Milwaukee, WI) dissolved in 10 cc of normal saline. Three control rats received an intraperitoneal injection of 10 cc normal saline. Thirty-six hours after injection, symmetric and asymmetric-sequence (4 ms) images were obtained under light sedation with sodium pentobarbital. Immediately after imaging, the rats were sacrificed and frozen sections obtained from a constant region of the right lobe of the liver of each rat and stained with oil red O. For each pair of symmetric- and asymmetric-sequence (4 ms) images, the signal intensity from an identical region of the liver was integrated and the difference signal D was calculated according to equation 1.

Measurements of the NMR signal decay due to reversible tissue-induced dephasing were made for rat liver, inflated lung, retroperitoneal fat, and liquid corn oil by two independent methods. In the first experiment, a set of four glass tubes (11 mm I.D.) containing each of the above samples was immersed in water and imaged in cross section. Images were obtained using symmetric and asymmetric (2, 4, and 6 ms) sequences. In each image, the signal intensity of an identical region from the center of each sample (corresponding to approximately 50% of the cross-sectional area of the tube) was integrated and the asymmetric-sequence signal intensity, expressed as a fraction of the symmetric-sequence signal intensity (1-D, see equation 1), was plotted as a function of increasing sequence asymmetry (a).

In a second experiment, a different approach was taken; reversible tissue-induced dephasing was determined from recorded free induction decays (FIDs) which were corrected for magnet inhomogeneity and irreversible signal loss. The FID of the NMR signal after a 90° pulse was recorded with 32 averages for similar but smaller samples of corn oil, rat liver, retroperitoneal fat, inflated lung and distilled water ( $T_2$  of distilled water > 2s). The FID of water was used to correct for magnet inhomogeneity (see  $f_{mag}$  defined in A, Fig. 2). In each case, the sample occupied the same volume and geometry in precisely the same location within the most homogenous portion of the magnetic field. The total decay rate of the observed FIDs includes contributions from reversible tissue-induced dephasing as well as from magnet inhomogeneity and irreversible processes. In order to determine the contribution of reversible tissue-induced dephasing, two assumptions were made: (1) the decay due to irreversible dephasing is described by a single exponential whose time constant,  $T_2$ , can be correctly determined for each tissue by observing the rate of decline of the spin echo amplitudes in a Carr-Purcell sequence<sup>10</sup>; and (2) the decay due to magnet inhomogeneities is constant from sample to sample and is the only significant source of dephasing (during the first 11 ms) in the sample of distilled water, within which no static sample-induced magnetic inhomogeneities should exist. For each sample, that portion of signal decay attributable to reversible tissue-induced dephasing was determined by correcting for the signal loss due to magnet inhomogeneity and to irreversible processes, at 1 ms intervals from 0 to 11 ms (Fig. 2). This corrected FID is different from the conventional FID, which is well known to be similar in shape to the spin echo. In contrast, our corrected FID is identical in shape to the *envelope* of the heights of spin echoes obtained at different asymmetry (a).

For inflated lung and for fat, we generated empirical mathematical expressions that fit the experimental data. Although

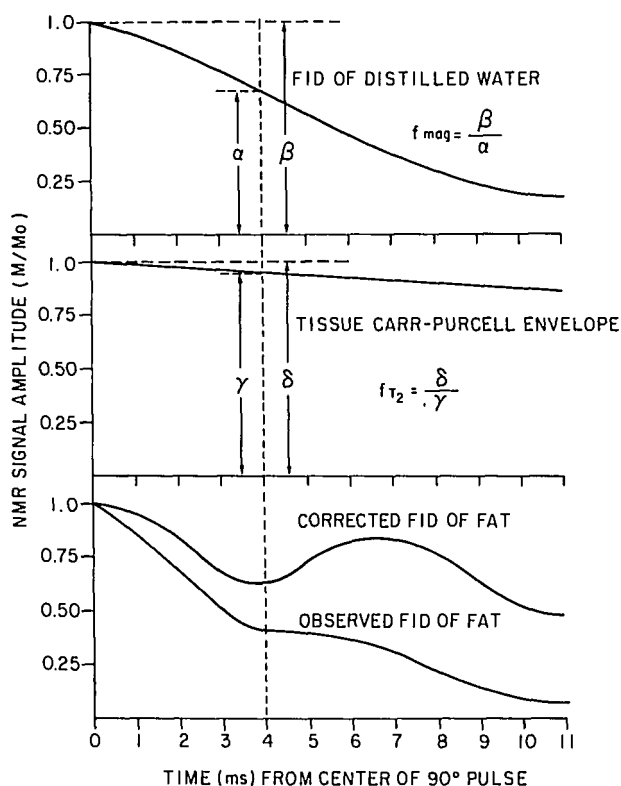


Fig. 2. Correction of the observed NMR signal amplitude for signal losses due to magnet inhomogeneity and irreversible processes. The observed NMR signal amplitude was corrected at each point in time by multiplying the observed signal amplitude by the correction factors  $f_{mag}$  and  $f_{T_2}$  according to  $M_{corrected} = M_{observed} \times f_{mag} \times f_{T_2}$ . The observed and correct NMR signal amplitude curves (FIDs) are displayed in panel C. The correction factor ( $f_{mag}$ ) for magnet inhomogeneity is defined in panel A and was determined from the experimentally recorded FID of the sample of distilled H<sub>2</sub>O. The correction factor ( $f_{T_2}$ ) for irreversible NMR signal loss is defined in panel B and was determined experimentally (Carr-Purcell technique) for each specific tissue.

different chemically shifted species within a sample may have different line widths and thus different  $T_2$  values, the assumption made does not induce a significant error. For example, in the worst possible case in which the sample contains equal fractions of alkyl (-CH<sub>2</sub>-) and hydroxyl (-OH) protons, the resultant error in the final magnetization value is only 5%, since  $T_2$  (tissue water)  $\approx$  40 ms and  $T_2$  (lipid)  $\approx$  80 ms. Under the conditions of our study in which the samples studied were either mostly water (liver, lung) or mostly lipid (fat), the resultant error is less than 2% (less than the noise of our measurements).

Spectra of liquid corn oil, partially hydrogenated corn oil, rat liver, and rat retroperitoneal fat were obtained at 300 MHz (7.1 tesla) using a Varian SC 300 spectrometer (Varian Corp., Palo Alto, CA). Samples were placed in a 5-mm probe and spun at 20 rpm. All spectra were obtained at 37° C, except the partially hydrogenated vegetable oil in which case spectra were obtained at 5° C intervals from 26° to 56° C.

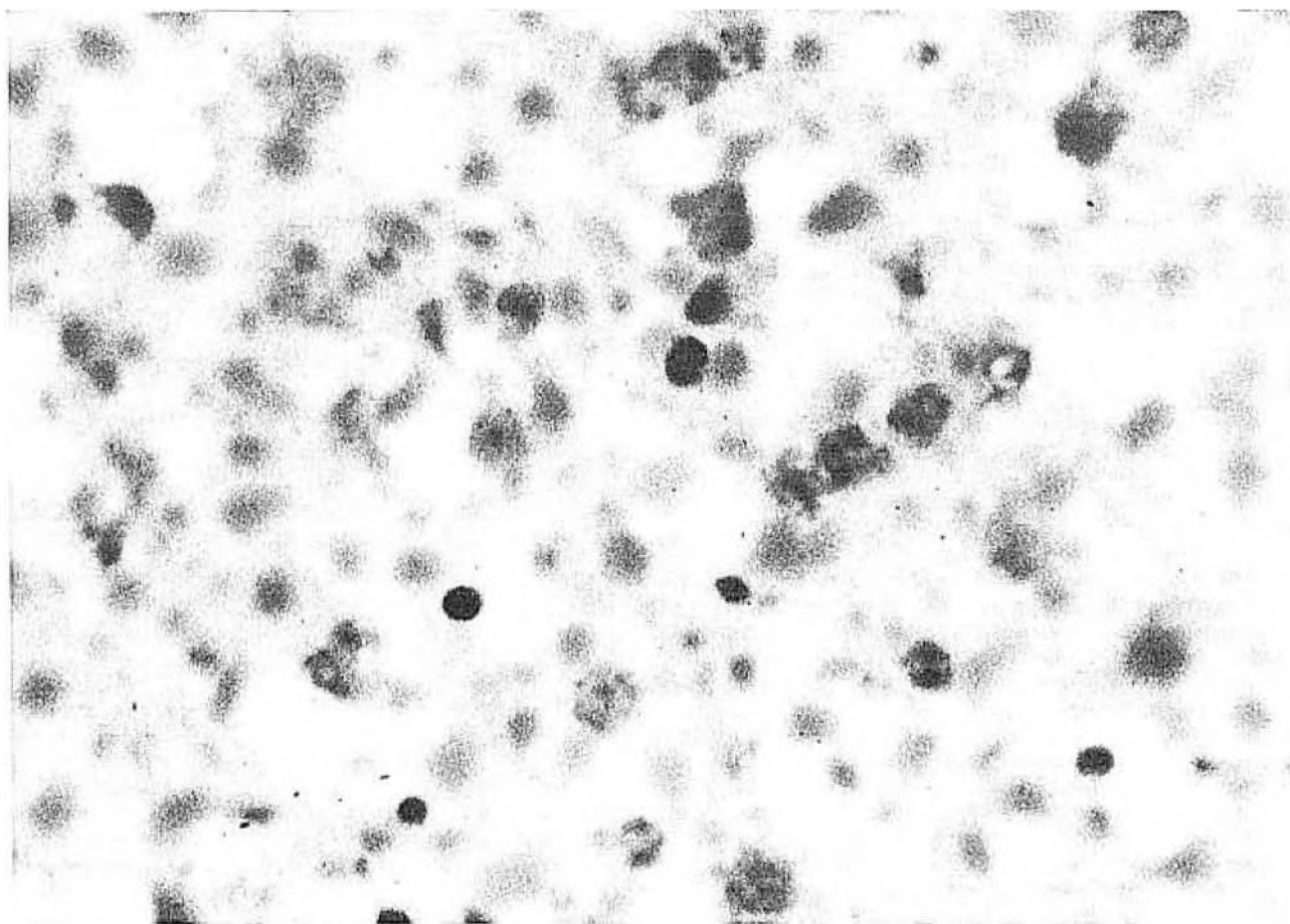


Fig. 3A. Frozen section stained with oil red O from the liver of a rat 36 hours after treatment with ethionine showing many fat vacuoles (magnification approximately  $\times 2000$ ). Number of cell nuclei identical to that of Fig. 3B.

### Results

In all the rats that received ethionine, histologic specimens revealed significant steatosis (Fig. 3A), whereas no accumulation of lipid was demonstrated in the controls (Fig. 3B). In the rats treated with ethionine (Fig. 3C) but not in controls (Fig. 3D), the presence of fat in the liver was apparently by its brightness in the subtraction images obtained from paired symmetric and asymmetric (4 ms) spin echo sequences. The mean ( $\pm$  S.D.) difference signal D (equation 1) from the livers of the four rats treated with ethionine was  $0.193 (\pm 0.022)$  compared with  $0.014 (\pm 0.022)$  for the three controls ( $P < .0005$ ). The mean signal intensity ( $\pm$  S.D.) from the liver in symmetrical sequence images was  $95.0 (\pm 5.0)$  units for treated animals and  $83.7 (\pm 7.2)$  units for the controls; the difference between the two groups was not statistically significant ( $P = .07$ ).

The spectrum of liquid corn oil (Fig. 4A) contains very narrow chemically shifted resonance lines whose widths

vary from 18 to 37 Hz (0.06–0.11 ppm). Partially hydrogenated corn oil below  $47^\circ\text{C}$  is a semisolid and has only two broad ( $\approx 400$  Hz, 1.3 ppm) resonance lines (Fig. 4B) which, upon melting (at  $47$ – $48^\circ\text{C}$ ), become motionally narrowed with the appearance of multiple resonance lines with widths of 47–55 Hz (0.16–0.19 ppm) (Fig. 4C). Retroperitoneal fat at  $37^\circ\text{C}$  has a spectrum with line widths intermediate between liquid corn oil and semisolid partially hydrogenated corn oil (120 Hz, 0.4 ppm) (Fig. 4D). The spectrum of liver consists of a single 57 Hz (0.19 ppm) wide resonance line (Fig. 4E). In all spectra, the chemical shift between the resonance lines of the hydroxyl (-OH) and the major alkyl (-CH<sub>2</sub>-) protons was 4.0 ppm.

Figure 5 shows paired symmetric- (Fig. 5A) and asymmetric-sequence (4 ms) (Fig. 5B) and subtraction (Fig. 5C) images of the tubes containing liquid corn oil, inflated lung, retroperitoneal fat, and liver. Compared with the symmetric sequence, the asymmetric-sequence (4 ms) image signal

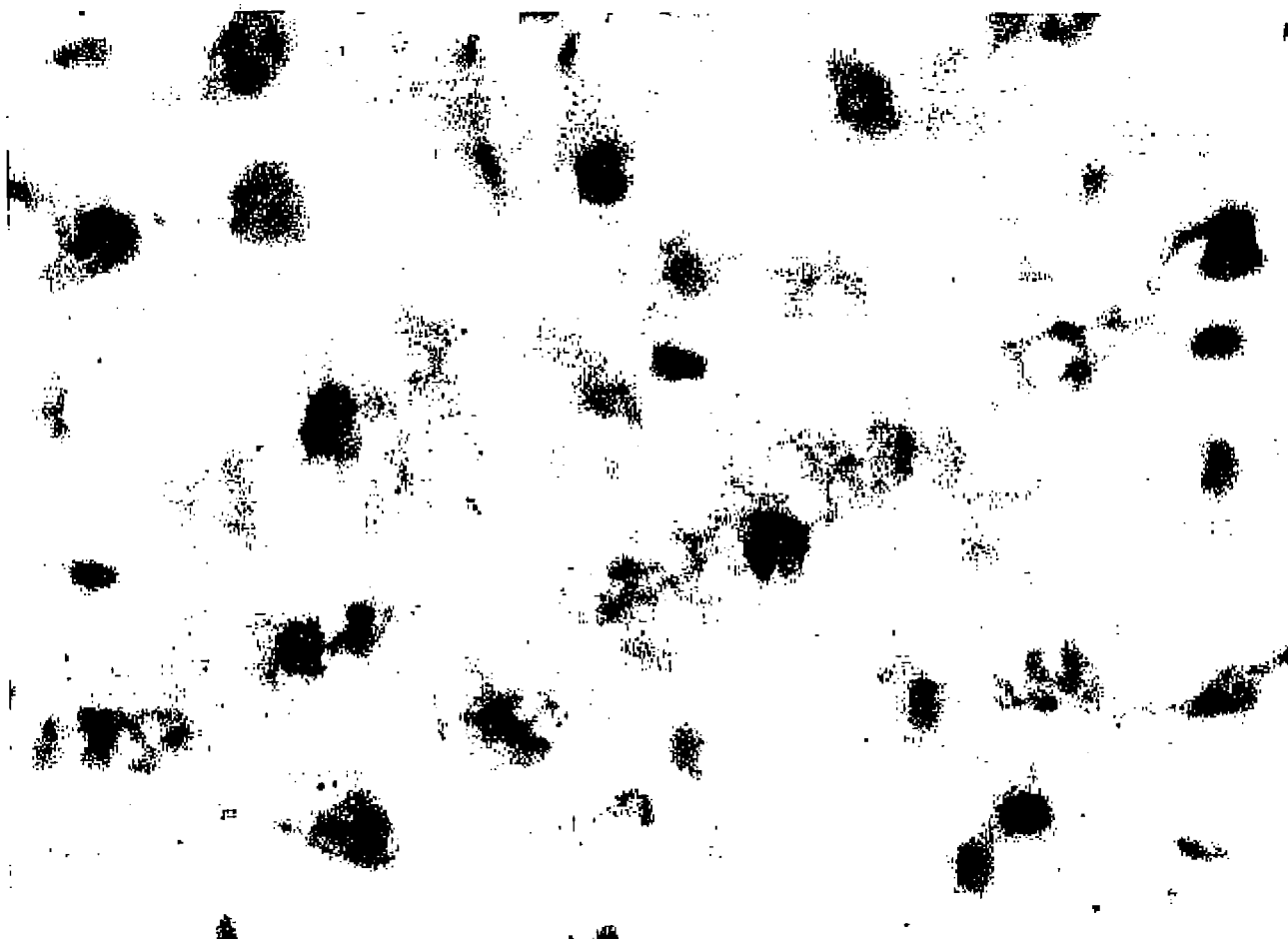


Fig. 3B. Frozen section stained with oil red O from the liver of a control rat. No fat vacuoles are present (magnification approximately  $\times 2000$ ). The only identifiable structures are cell nuclei.

intensity is decreased for the oil, inflated lung, and fat but not for liver nor for the water in which the glass tubes were immersed.

The corrected FIDs (describing only the decay of the NMR signal due to reversible tissue-induced dephasing) for similar samples are shown in Fig. 6. Superimposed upon the corrected FID for each sample are the corresponding asymmetric-sequence signals (open circles) expressed as fractions (1-D) of the symmetric-sequence signals. A comparison of the measurements of the signal decay due to reversible tissue-induced dephasing obtained by these two different methods (corrected FID and asymmetric sequence cross-sectional images) yielded a correlation coefficient ( $r$ ) of .96 ( $P < .001$ ). The decay curves in Fig. 6 are clearly not described by simple exponentials. The curve for liver is nearly flat indicating no significant contribution of reversible tissue-induced transverse dephasing. The decay curve for inflated lung was fit ( $r = .999$ ) by the expression

$$M = M_0 \exp [-(t/T_2^*)^{3/2}], \quad (2)$$

where  $t$  equals the time elapsed from the center of the  $90^\circ$  pulse and  $T_2^*$  equals 4.8 ms. Equation 2 corresponds to the Fourier transformation of a single line intermediate in shape between Lorentzian and Gaussian. The curve for retroperitoneal fat was fit ( $r = .992$ ) by the expression:

$$M = M_0 (0.269 \cos \Omega t + 0.731)^{1/2} \exp [-(t/T_2^*)^2], \quad (3)$$

where  $T_2^* = 16$  ms and  $\Omega = 2\pi/(7.3$  ms) (Fig. 7).

#### Discussion

The decay of the FID is, in general, due to contributions from several sources: external magnet inhomogeneities,  $T_2$  effects arising from irreversible processes, and reversible tissue-induced dephasing. Since reversible tissue-induced dephasing appears to be characteristic of inflated lung and fat, it can be used as a means of identifying these tissues. Therefore, techniques that isolate the contribution of

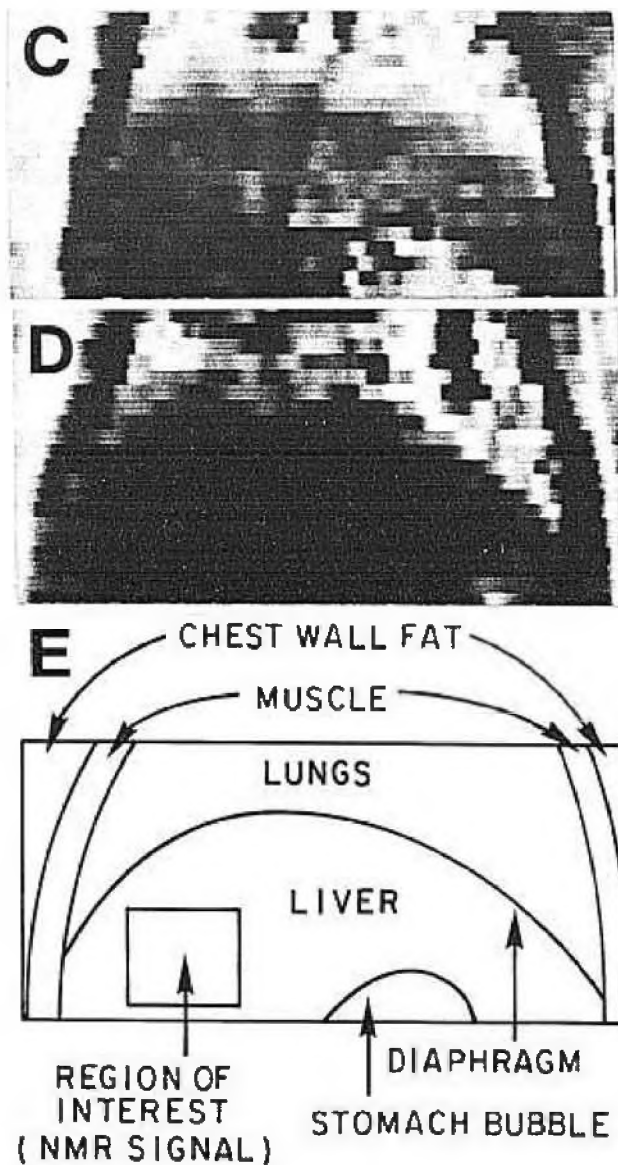


Fig. 3(C). Coronal NMR subtraction image obtained from paired symmetric and asymmetric (4 ms) images of a rat 36 hours after treatment with ethionine (same rat as in Fig. 3A). The lower portion of chest and the upper portion of abdomen are shown. (D) Coronal NMR subtraction image obtained from paired symmetric and asymmetric (4 ms) images of a control rat (same rat as in Fig. 3B). The lower portion of chest and upper portion of abdomen are shown. (E) Line drawing of organs. The stomach bubble, usually visible in subtraction images, can be seen (we think) because of its foamy contents.

reversible tissue-induced dephasing are desirable. The contribution from reversible tissue-induced dephasing dominates the FID of fat and inflated lung, in contrast to tissues such as liver. As a result, it is easy to isolate the reversible tissue-induced dephasing by removing the contributions

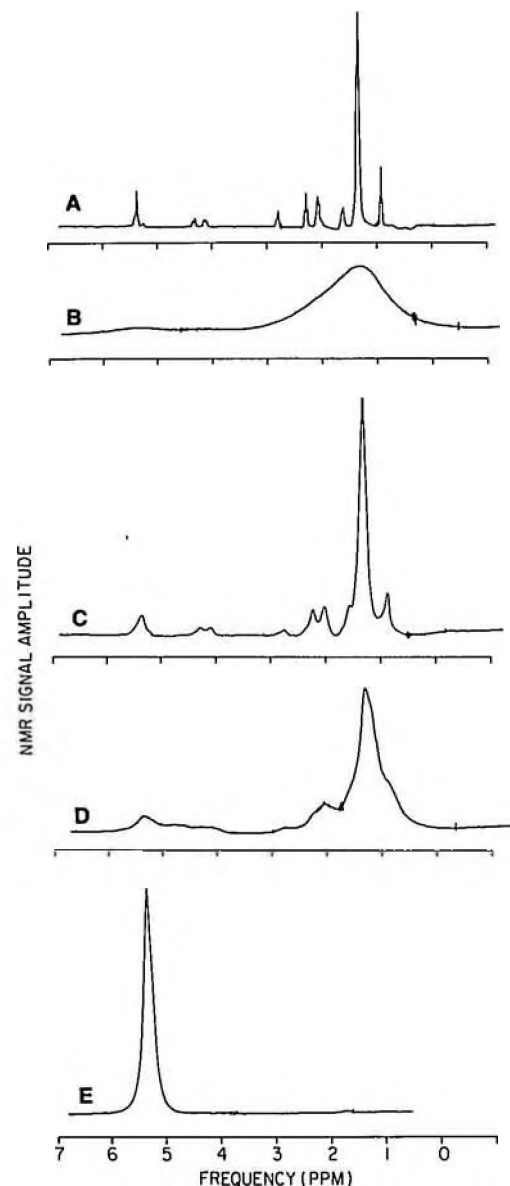


Fig. 4. High resolution (300 MHz) spectra of liquid corn oil (A), partially hydrogenated corn oil below 47° C (semisolid) (B), and above 48° C (liquid) (C), retroperitoneal fat (D), and liver (E).

from magnet inhomogeneities (external) and irreversible processes. We show that this corrected FID is virtually identical to the NMR signal magnitude as a function of asymmetry (a). The time that characterizes this decay due to reversible tissue-induced dephasing is  $T_2^*$ .<sup>6</sup> Within experimental error,  $T_2^*$  obtained from the corrected FID is identical to that obtained from the asymmetric image (Fig. 6). A record of NMR signal intensity as a function of asymmetry (a) provides a rapid and more direct means of studying

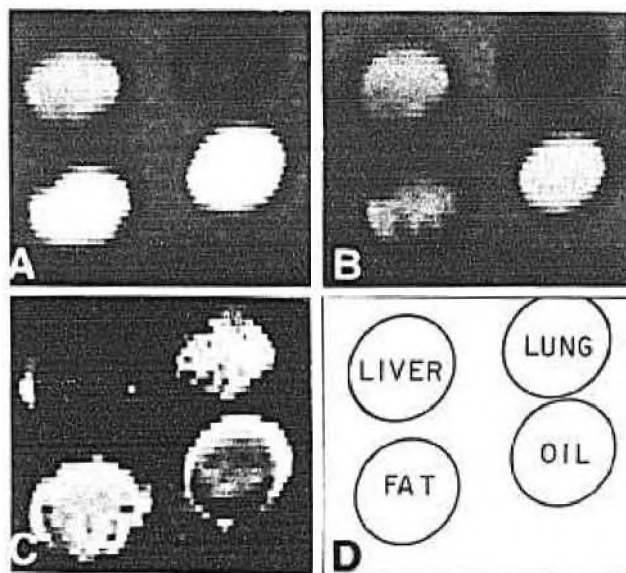


Fig. 5. Symmetric (A), asymmetric (4 ms) (B), and subtraction (C) images of four tubes containing rat liver, inflated rat lung, rat retroperitoneal fat, and liquid corn oil (all tubes immersed in water).

reversible tissue-induced dephasing than that provided by correcting the FID.

We have reported previously that the FID of inflated lung is markedly shortened when compared with airless lung and liver, suggesting that, in the inflated state, lung is associated with reversible tissue-induced dephasing<sup>6,7</sup>; our data indicate that this finding may reflect the influence of air-tissue interfaces upon the internal magnetic field (see Introduction). Since no air-tissue interfaces are present in bulk oil or fat and since the observed NMR signal for fat has a different waveform (equation 3) from that of inflated lung (equation 2), the source of the reversible tissue-induced dephasing in fat must be different from that in inflated lung. Based on the observations reported herein and presented in preliminary form,<sup>11</sup> we suggest that the reversible tissue-induced dephasing in fat arises from chemically shifted resonance lines and incompletely averaged local dipolar interactions in the presence of chemically shifted resonance lines.

The envelope of an FID is the magnitude of the Fourier transform of its frequency spectrum<sup>12</sup> and can be expressed in the general case by

$$M = \left| \sum_j C_j e^{i\omega_j t} \right|, \quad (4)$$

where  $C_j$  is the Fourier coefficient and  $\omega_j$  is the Larmor frequency of the  $j^{\text{th}}$  resonance line. Under conditions of low

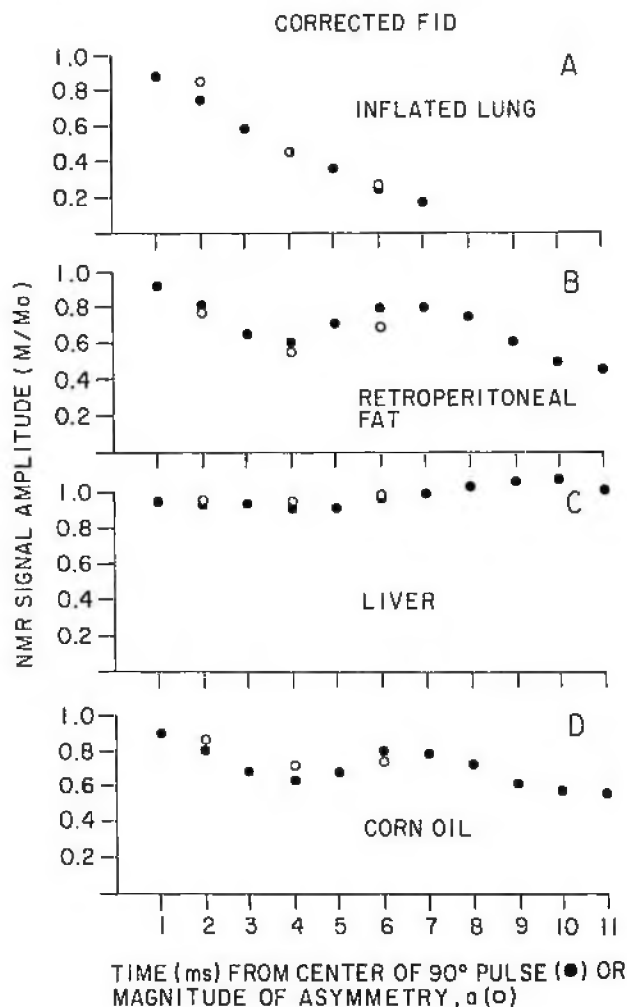


Fig. 6. Decay of NMR signal intensity due to reversible tissue-induced dephasing for inflated rat lung (A), rat retroperitoneal fat (B), rat liver (C), and liquid corn oil (D). Corrected FIDs shown with solid circles and corresponding asymmetric image signal intensity fractions (1-D, see text) computed from images of similar samples shown as open circles. Half-filled circles represent superimposed open and closed circles.

resolution, the frequency spectrum of tissue appears as essentially two broad resonance lines of water and alkyl protons. For the case in which the frequency spectrum consists of two very narrow resonance lines separated by a frequency  $\Delta\omega$ , equation 4 can be written as

$$M = (A^2 + B^2 + 2AB \cos \Delta\omega t)^{1/2} \quad (5)$$

where  $A$  and  $B$  are the integrals of the two resonance lines. The Fourier transform of this idealized spectrum (equation 5) has the same form as the coefficient of  $\exp[-(t/T_2)^2]$  of



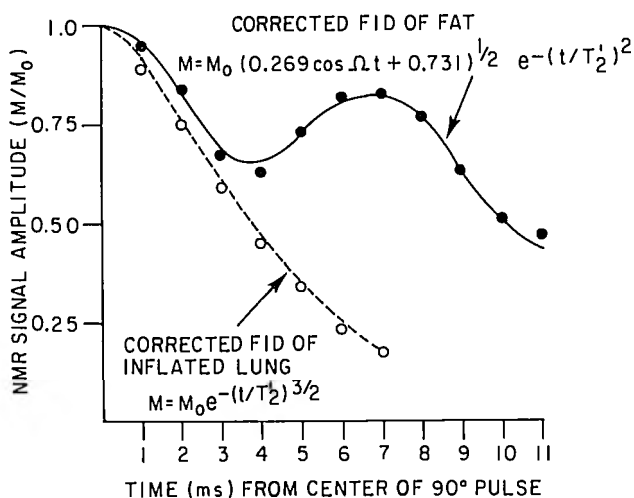


Fig. 7. Empirical expressions describing the magnitude of the NMR signal as a function of time for inflated rat lung (broken line) and rat retroperitoneal fat (solid line). For explanation, see Discussion. Experimental data points (corrected FIDs) for inflated rat lung (open circles) and rat retroperitoneal fat (solid circles) are plotted with the corresponding empirical curves.

equation 3. The frequency difference  $\Delta\omega$  in equation 5 thus corresponds to the fit parameter  $\Omega$  in equation 3. In spite of the fact that the spectrum of fat (Fig. 4) is more complicated than the two sharp line spectrum assumed for the theoretical generation of equation 5, we observed a period of oscillation (6.3 ms) which was within 1 ms of the predicted 7.3 ms. Since the spectrum of fat does not consist of two sharp lines but contains broad peaks between the alkyl and hydroxyl peaks (Fig. 4D), the period of oscillation should, in fact, be greater than 6.3 ms, as our data indicate. Our model appears, therefore, to provide a satisfactory description of reversible tissue-induced dephasing in fat.

The predicted periods of oscillation of 1.5 T (64 MHz) and 0.35 T (15 MHz) are 4 and 18 ms, respectively. The terms A and B of equation 5 represent the integrals of the water and alkyl resonances and can be evaluated most easily at the half period where  $\cos \Delta\omega t = -1$ . This point in time corresponds to the first minimum of equation 3, as shown in Fig. 7. Under this condition, equation 5 becomes

$$M = |A-B| \quad (6)$$

and the fractions of the two peaks can be readily calculated. It is important to note however that, because of the absolute value in equation 6, unambiguous determination of which peak ( $-\text{OH}$  or  $-\text{CH}_2-$ ) predominates requires additional measurements.

In addition to the oscillation of the two "beating" peaks described by equation 5, a Gaussian factor appears in the empirical description of the corrected FID of fat (equation 3). We suggest that this arises because the frequency spectrum of tissue is not composed of two very narrow resonance lines. Rather, as is well known (and demonstrated in Fig. 4), the "alkyl" resonance is composed of the large line of the  $-\text{CH}_2-$  protons surrounded by smaller lines of other carbon protons in several other environments. Each of these lines is in turn broadened by as much as 40 to 120 Hz. The empirical value of 16 ms for the time constant  $T_2'$  corresponds to an effective line width of approximately 62 Hz or 1.6 ppm at 40 MHz. Thus, the oscillations of the two beating frequencies become damped to  $1/e$  of the initial amplitude at  $T_2'$  (16 ms for fat at 40 MHz).

This method appears to be capable of detecting in vivo liver steatosis noninvasively. A correlation between signal intensity and triglyceride content in the livers of rats treated with ethionine has been reported<sup>13</sup>; however, the signal image intensity measurements were reported to increase only minimally despite massive increases in triglyceride content. Because signal intensity measurements are dependent upon  $T_1$  and  $T_2$ , which in liver vary in both normal and pathologic states, it is doubtful that signal intensity data alone can be a reliable indicator of the presence and degree of hepatic steatosis. We also noted a higher mean signal intensity in the rats treated with ethionine, than in the control rats; however, the difference did not reach the 5% level of statistical significance. In contrast, the subtraction liver images obtained from paired symmetric and asymmetric (4 ms) sequences from rats with fatty livers were significantly different from those obtained from normal controls ( $P < .0005$ ). Although further studies are needed, we expect that when correctly obtained, paired symmetric- and asymmetric-sequence images will provide information that is both specific and quantitative for hepatic steatosis.

In summary, we have shown that symmetric and asymmetric spin echo sequences can be used to obtain proton spectral information in fat. When reversible tissue-induced dephasing is present (eg, in inflated lung and in fat), a new time constant  $T_2'$  quantitatively reflects the internal NMR line broadening. The presence of fat in the livers of rats with chemically induced steatosis was demonstrated quantitatively. Rather than producing a complete spectrum by Fourier analysis of a series of increasingly asymmetric sequence images, a single symmetric- and asymmetric-sequence image pair should allow calculation of  $T_2'$  for each pixel and may provide important diagnostic information without the extensive imaging time required for traditional spectroscopy. Since our small animal studies were carried out in a magnetic field inhomogeneity comparable to that of modern superconducting magnets, our technique for studying reversible tissue-induced dephasing should be as easily applied to whole body systems required for human study.



### References

1. Alfidi RJ, Haaga JR, El Youset SJ, et al. Work in progress. Preliminary experimental results in humans and animals with a superconducting, whole-body, NMR scanner. *Radiology* 1982;143:175-181.
2. Crooks L, Arakawa M, Hoenninger J, et al. Work in progress. Nuclear magnetic resonance whole-body imager operating at 3.5 KGauss. *Radiology* 1982;143:169-174.
3. Bottomley PA. NMR imaging techniques and applications: A review. *Rev Sci Instrum* 1982;53:1319-1337.
4. Edelstein WA, Bottomley PA, Hart HR, Smith LS. Signal, noise, and contrast in nuclear magnetic resonance (NMR) imaging. *J Comput Assist Tomogr* 1983;7:391-401.
5. Pykett IL, Rosen BR. Nuclear magnetic resonance: In vivo proton chemical shift imaging. *Radiology* 1983;149:1976.
6. Ailion DC, Case TA, Blatter DD, et al. Applications of NMR spin imaging to the study of lungs. *Bull Mag Res* 1984;6:130-139.
7. Morris AH, Blatter DD, Case TA, et al. A new nuclear magnetic resonance property of lung. *J Appl Physiol* 1985;58(3):759-762.
8. Crooks L. Selective irradiation line scan techniques for NMR imaging. *IEEE Trans Nucl Sci NS* 1980;27(3):1239-1244.
9. Farber E, Simpson MV, Tarver H. Studies on ethionine. I. The interference with lipide metabolism. *J Biol Chem* 1950;182:91-99.
10. Carr HY, Purcell EM. Effects of diffusion on free precession in nuclear magnetic resonance experiments. *Phys Rev* 1954;94:630-638.
11. Ailion DC, Blatter DD, Case TA, Morris AH, Cuttillo AG, Durney CH. Asymmetric imaging. Proceedings of the XXIIInd Congress Ampere, Zurich: Zurich Ampere Committee, University of Zurich, 1984:510-511.
12. Gadian DG. Nuclear magnetic resonance and its applications to living systems. Oxford: Clarendon Press, 1982:97.
13. Stark DD, Bass NM, Moss AA, et al. Nuclear magnetic resonance imaging of experimentally induced liver disease. *Radiology* 1983;148:743-751.

---

### Announcements

**Chest Radiology—Update and Review.** December 2-6, 1985, Hotel Del Coronado, Coronado, CA. Accreditation: 20 hours Category I. Fee: \$400; \$250 for residents/fellows. For information, contact Dawne Ryals, Ryals and Associates, PO Box 610203, DFW Airport, TX 75261-0203. (214) 659-9590.

**Computed Tomography Head to Toe.** December 16-21, 1985. Grand Hyatt New York, NYC. Accreditation: 39 Category I. Registration \$525. For information, contact NYU Medical Center Post-graduate Medical School, 550 First Avenue, New York, NY 10016. (212) 340-5295.

**7th Annual Winter Conference in the High Sierras.** February 2-7, 1986, Caesar's Tahoe Hotel, Lake Tahoe, Nevada. Accreditation: \$25 hours Category I. Registration: \$395; daily registration \$115.

For further information, contact American College of Medical Imaging, PO Box 27188, Los Angeles, CA 90027. (213) 275-1393.

**UCSD Radiologic Imaging and Intervention Course.** February 3-7, 1986, Hotel Intercontinental, San Diego CA. Accreditation: 20 hours Category I. Registration: \$400. For information, contact Eric vanSonnenberg, Md, PO Box 61203, DFW Airport, TX 75261. (214) 659-9590.

**Thoracic Imaging—1986.** February 17-20, 1986, Newporter Beach Resort Hotel, Newport Beach, CA. Sponsored by The Society of Thoracic Radiology. Registration: \$425 (postgraduate course); \$499 (course and scientific session); \$250 Residents/Techs/Fellows/Military; \$100 (Scientific Session only). For information, contact Dawne Ryals, Ryals and Associates, PO Box 610203, DFW Airport, TX 75261-0203. (214) 659-9590.